

COMBINATION OF CLADDING PROCESSES WITH SUBSEQUENT HOT FORMING AS A NEW APPROACH FOR THE PRODUCTION OF HYBRID COMPONENTS

L. Budde¹, P. Merkel², V. Prasanthan³, S. Bährisch⁴, M. Y. Faqiri⁵, M. Lammers¹, M. Stonis², J. Hermsdorf¹, T. Hassel⁵, J. Uhe⁴, B.-A. Behrens^{4,2}, B. Breidenstein³, L. Overmeyer¹

¹Laser Zentrum Hannover e.V., Hannover, Germany

²IPH – Institut für Integrierte Produktion Hannover gGmbH, Hannover, Germany

³Institute of Production Engineering and Machine Tools, Leibniz University Hannover, Garbsen, Germany

⁴Institute of Forming Technology and Machines, Leibniz University Hannover, Garbsen, Germany

⁵Institute of Materials Science, Leibniz University Hannover, Garbsen, Germany

Abstract

A new process chain for the manufacturing of load-adapted hybrid components is presented. The "Tailored Forming" process chain consists of a deposition welding process, hot forming, machining and an optional heat treatment. This paper focuses on the combination of laser hot-wire cladding with subsequent hot forming to produce hybrid components. The applicability is investigated for different material combinations and component geometries, e.g. a shaft with a bearing seat or a bevel gear. Austenitic stainless steel AISI 316L and martensitic valve steel AISI HNV3 are used as cladding materials, mild steel AISI 1022M and case hardening steel AISI 5120 are used as base materials. The resulting component properties after laser hot-wire cladding and hot forming such as hardness, microstructure and residual stress state are presented. In the cladding and the heat-affected zone, the hot forming process causes a transformation from a welding microstructure to a fine-grained forming microstructure. Hot forming significantly affects the residual stress state in the cladding the resulting residual stress state depends on the material combination.

Keywords: Laser hot-wire cladding, Cladding, Hot forming, Residual stress, Microstructure, Hardness, Tailored Forming

Introduction

Metallic claddings are used in a wide range of applications to protect the component from environmental influences or high loads. The cladding material is adapted to the type of load applied to the hybrid component. Claddings can protect the base material from chemical, physical and/or tribological stresses. For example, a cladding of stainless steel can protect the base material from corrosion, while materials with high hardness can protect the base material from abrasive wear [1]. Due to the hybrid design with load-adapted claddings, the component can be made from low-cost mild steel and the higher-priced, high-strength or corrosion-resistant alloys are only used selectively in stressed component areas. Accordingly, material costs can be reduced by such resource-efficient material selection.

State of the art

A number of processes are available for the application of claddings, which differ in the properties produced. For the manufacturing of claddings with a thickness from 0.5 mm to several millimeters, cladding processes based on welding are used. In most cases, the application of a single weld seam is not sufficient to achieve a wide cladding. By applying overlapping weld seams, a sufficiently wide cladding is produced [2]. The surface of the cladding has a high waviness and roughness, which is why machining is usually used after cladding to achieve the application-specific surface quality [3]. In order to keep the machining effort as low as possible, a number of investigations were carried out and models were developed which predict the waviness perpendicular to the welding direction depending on process parameters of the deposition welding process and can thus be used to optimize the rework effort [4–6].

The microstructure and hardness of additively manufactured parts can be adapted to the application by subsequent heat treatment. Junker et al. investigated the influence of heat treatment strategies on additively manufactured parts of hot work tool steel and compared the results to conventionally manufactured samples [7]. The hardness and compression strength after deposition welding was similar to those of conventionally manufactured samples after hardening but the yield strength was lower. After heat treatment, consisting of austenitization, quenching and three tempering cycles, the mechanical properties of the additively manufactured samples were similar to those of the conventionally manufactured sample. Tempering without pre-austenitization of the additively manufactured sample led to an improvement of the mechanical properties exceeding those of conventionally manufactured samples.

Hafenecker et al. investigated the cold forming of additively manufactured cylinders of AISI 316L and of Ti-6Al-4V by a cup backwards-extrusion process [8]. The cylinders were manufactured by a laser-based powder bed fusion process. The surface roughness of the lateral surface of AISI 316L samples was reduced by 90 % by cold forming and geometric shapes like sharp edges were improved. Due to the low formability, no improvement could be seen for the Ti-6Al-4V samples.

In laser deposition welding, residual stresses occur due to the high temperature gradients and the rapid cooling of the melt pool, which can lead to distortion or crack formation depending on the component geometry and material combination. High tensile residual stresses usually occur near the surface, which can have a negative effect on the service life of the component. Various strategies can be used to reduce residual stresses or to selectively set beneficial residual stresses. Beneficial residual stresses are those that counteract load-induced stresses in the component. For example, by inducing compressive residual stresses into the surface and subsurface area, the service life of rolling element bearing raceways can be improved. The tensile residual stresses can be shifted towards the compressive range by processes that apply compressive mechanical loads like laser shock peening, deep rolling, hard turning or grinding. In the case of the latter two processes, it should be noted that additional tensile residual stresses can be induced by thermal effects. Residual stresses can be reduced by preheating the substrate or by subsequent heat treatment [9].

In addition to the aforementioned processes of cold forming, as well as hardening and machining of clad components to improve their properties, hot forming can also be used. For hot forming, components are heated above the material specific recrystallisation temperature. After forming, the component is cooled, which can be done in ambient air or liquids, such as oil or water. Microstructure, residual stress state and hardness of the component are influenced during hot forming. Compared to cold forming, higher degrees of forming can be achieved, by which a higher change in shape of the component is reached [10].

For the assessment of the suitability of the hot forming process for the further processing of clad components, knowledge of the influence of the hot forming process on the surface and subsurface properties is required. Hardness, residual stress state and microstructure of the cladding material have a significant influence on the application behaviour of hybrid components and will therefore be examined in detail in this study.

Aims and perspective

A process chain for the manufacturing of hybrid components consisting of a joining or cladding process, a hot forming process, a machining process and, if necessary, heat treatment is referred to as a Tailored Forming process chain. In this study, the focus is on the first two process steps of the Tailored Forming process chain, cladding and hot forming. In the following, the findings on resulting surface and subsurface properties after hot forming of semi-finished products clad by means of laser hot-wire cladding are presented using the example of two geometries, a shaft with bearing seat and a bevel gear, and different material combinations. Hence, the following scientific questions have to be answered:

1. How does the hot forming process affect the surface and subsurface properties of the hybrid component regarding
 - a. Hardness
 - b. Microstructure
 - c. Residual stress state
 - d. Cladding layer distribution?

2. How does hot forming affect the amount of machining required to achieve the final geometry of the hybrid part?

Hybrid components of the aforementioned geometries are manufactured for the investigation of the research questions. Various material combinations are used for this purpose.

Materials and Methods

Two different component geometries are considered for the investigation. A cylindrical shaft is used as the base material for the production of hybrid shafts with bearing seats. The cladding is applied in the area of the bearing seat. A shaft with a conical shape is used for the manufacturing of hybrid bevel gears. The cylindrical shafts are made of mild steel AISI 1022M or case hardening steel AISI 5120 while the shafts with conical shape are made of AISI 1022M. Figure 1 shows an overview of the process steps that were investigated, as well as the component geometries and material combinations. The base material is shown in Figure 1 (A₁) and (B₁), the component geometry after cladding is shown in Figure 1 (A₂) and (B₂) and the hybrid component after hot forming is shown in Figure 1 (A₃) and (B₃). The process steps and material selection are explained in detail below.

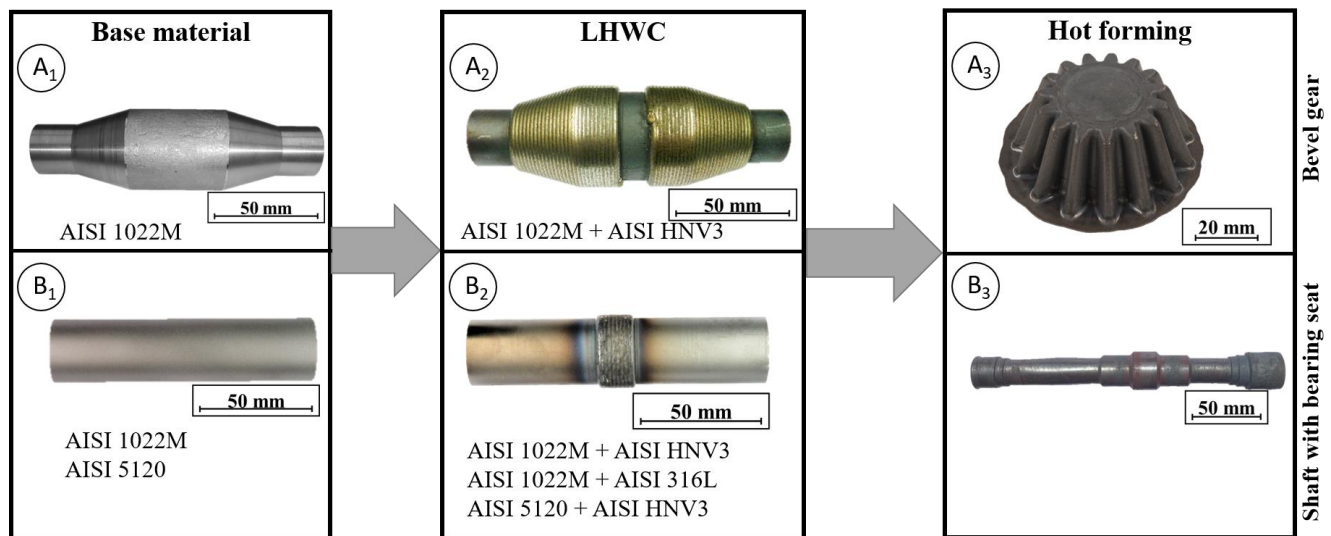


Figure 1: Overview of the investigated process steps, material combinations and geometries: (A₁) base material for bevel gear, (B₁) base material for shaft with bearing seat, (A₂) hybrid semi-finished part for bevel gear, (B₂) hybrid semi-finished part for shaft with bearing seat, (A₃) hybrid bevel gear after hot forming, (B₃) hybrid shaft with bearing seat after hot forming

The hybrid semi-finished parts are manufactured by laser hot-wire cladding (LHWC). For this purpose, the MK-II coaxial deposition welding head, manufactured by Laser Zentrum Hannover e.V., is used. In this welding head, the laser beam is split into four partial beams and deflected outwards. The partial beams are reflected by mirrors and converge again into one common spot. A hot current source is used to preheat the welding wire. A diode laser is used as the laser beam source. The base material is clamped in a rotary axis for the cladding process. By superimposing rotational movement and linear movement of the shaft and the processing head, spiral weld seams are applied to the shafts. The experimental setup is shown in Figure 2. Two different cladding materials are investigated. The AISI 316L austenitic stainless steel and the AISI HNV3 martensitic valve steel are used for the experiments. The AISI 316L stainless steel is characterized by excellent corrosion resistance, but has comparatively low strength. The material AISI HNV3 is characterized by high hardness and is used particularly in workpiece areas subject to high mechanical loads. The cladding materials investigated have different coefficients of thermal expansion. The mean coefficient of thermal expansion of AISI 316L between 20 and 400 °C is $17.5 \cdot 10^{-6} \text{ K}^{-1}$, which is significantly higher than the coefficient of thermal expansion of AISI 1022M ($14.1 \cdot 10^{-6} \text{ K}^{-1}$) and AISI HNV3 ($11.8 \cdot 10^{-6} \text{ K}^{-1}$).

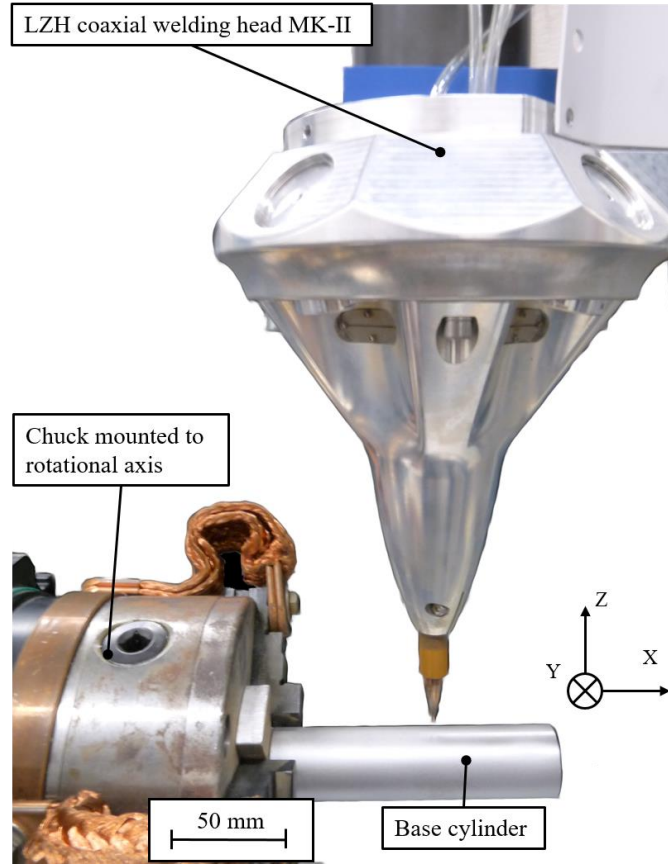


Figure 2: Experimental setup for laser hot-wire cladding

In order to study the effect of the forming process on the residual stress formation, shafts of the material combination AISI 1022M and AISI HNV3 are manufactured and compared with shafts of the material combination AISI 1022M and AISI 316L. By this, the influence of the thermal expansion coefficient on the residual stress formation can be determined. The influence of the cooling strategy on the hybrid components is investigated using shafts with bearing seats with the material combination AISI 5120 and AISI HNV3. After hot forming, the hybrid shafts are cooled in air or quenched in water. The high-strength AISI HNV3 cladding is used to study the bevel gear. The chemical composition of the cladding and base materials are shown in Table 1.

Table 1: Chemical composition of the investigated materials [11–14]

	C	Si	Mn	P	S	Cr	Ni	Mo	Fe
AISI 1022M	0.18-0.23	≤0.4	0.30-0.90	≤0.03	≤0.015	≤0.30	≤0.30	≤0.08	Bal.
AISI 5120	0.17-0.22	≤0.4	1.10-1.40	-	≤0.035	1.00-1.20	-	-	Bal.
AISI HNV3	0.44	3.14	0.4	-	-	9.1	-	0.01	Bal.
AISI 316L	0.013	0.873	1.709	0.017	0.01	18.3	12.22	2.641	Bal.

The cylindrical shafts are provided with a cladding of two layers and the conical shafts are provided with claddings of four layers. The geometry of the conical shaft is symmetrical, so that two claddings can be applied on one conical shaft. This design reduces the amount of waste when cutting the clad conical shaft to size prior to die forging. Two bevel gears can be manufactured from one cone shaft in the subsequent forming process. An overview of the parameters used to generate claddings is given in Table 2. For some material combinations, the welding parameters were adjusted from the first to the subsequent layers due to the increase in temperature of the component. In these cases, both parameter values are given in the table.

Table 2: Parameters for LHWC of the hybrid parts with different material combinations

Parameter	Unit	Shaft with bearing seat			Bevel gear
		AISI 316L AISI 1022M	AISI HNV3 AISI1022M	AISI HNV3 AISI 5120	AISI HNV3 AISI 1022M
Laser power P_L	kW	2.1	2.1/1.95	2.1	1.5/1.35
Current (wire preheating) I	A	70	90/80	90/80	80
Wire feed rate v_w	m/min	2	2	2	2
Welding speed v_s	mm/min	1,200	1,200	1,000	1,200
Wire diameter d_w	Mm	1.0	1.0	1.0	1.0
Stickout l_w	mm	6.5	6	6.9	7.7
Shielding gas flow \dot{V} (Argon)	l/min	6	8	6	8
Laser beam source	-	LDM 3000-40			
Focal length (collimation unit) f_c	mm	100			63

After cladding, the cylindrical shafts are formed into shafts with a bearing seat by means of cross-wedge rolling (CWR). CWR is a preforming process in which the masses are redistributed along the axis [15]. Two wedge-shaped tools move in opposite directions and reshape the workpiece producing axially symmetrical geometries. The CWR module at the IPH – Institut für Integrierte Produktion gGmbH is a CWR machine with two flat tools. The velocity of the tools is set to 150 mm/s. The tools are preheated to 150 °C to reduce the loss of heat from the workpiece during forming. Prior to forming the workpiece is heated to 1,250 °C using an induction oven. The principle of CWR is shown in Figure 3. Hot forming is followed by cooling in air or quenching in water.

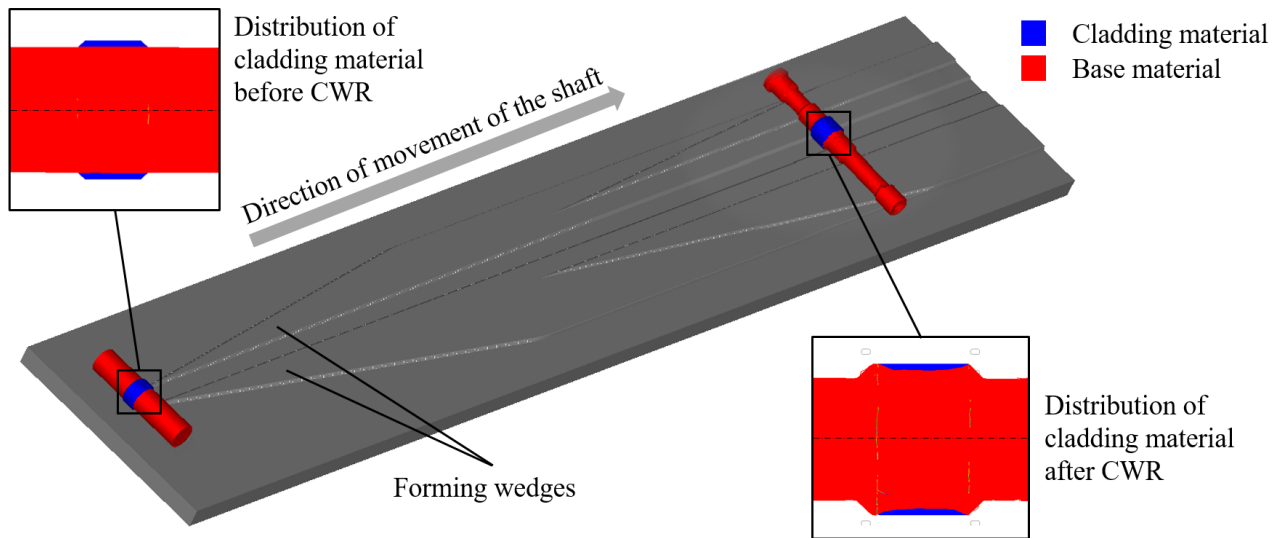


Figure 3: Process of cross-wedge rolling of hybrid parts

The conical shafts are formed into a bevel gear by die forging. The single-stage forming process is carried out using a screw press (Lasco SPR 500, 40 kJ). To prevent tool failure due to the fluctuating semi-finished volumes caused by the weld seams, the forging tool has a compensating system of closure plate in combination with disk springs. This design allows processing of welded semi-finished products without prior machining of the surface. The bottom die was heated to a temperature of 200 °C with a heating collar. Both, the lower die and the punch, were manually coated with a graphite-based lubricant (AirForge 5308 from Oelheld). To form the bevel gear, the semi-finished products are heated for 20 minutes to a temperature of 1,200 °C in a furnace with circulating air and inserted into the die. Directly after forming the glowing bevel gear was transferred to a process-integrated heat treatment which is explained in [16]. The experimental setup is shown in Figure 4.

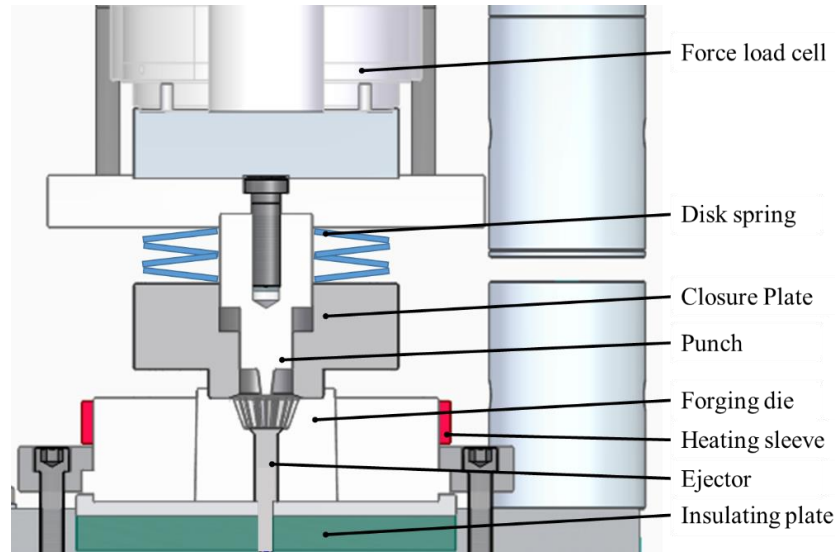


Figure 4: Experimental setup for die forging of hybrid bevel gears

Hardness, geometry and microstructure of the cladding are analyzed after LHWC and after hot forming in the cross-sections of the hybrid parts. Residual stress measurements are carried out by X-ray diffractometry using the $\sin^2\psi$ -method. For this purpose, a two-circle X-ray diffractometer by GE Inspection Technologies of the type Seifert XRD 3003TT is used. The measurements are made with $\text{Cr K}\alpha$ radiation with an applied high voltage of $U_A = 30 \text{ kV}$ and a current of $I_A = 35 \text{ mA}$. Residual stresses were determined in axial (σ_{\parallel}) and circumferential (σ_{\perp}) directions. For further details regarding the residual stress measurement, please refer to [17,18].

Results and Discussion

The cladding layer distribution after LHWC and after hot forming is shown in the cross-sections in Figure 5. CWR of the hybrid shafts reduces the thickness and increases the width of the cladding. The cladding covers the area of the bearing seat. As a result, the highly stressed area of the shaft is provided with a suitable material while the low-stressed component area is made of the low-cost material. The teeth of the bevel gear are formed by die forging. The core of the teeth consists of the base material with good ductility, and the surface area with the cladding material has high-strength properties. The tooth flanks, which are subjected to high loads during operation, thus have the necessary hardness for the loads during operation.

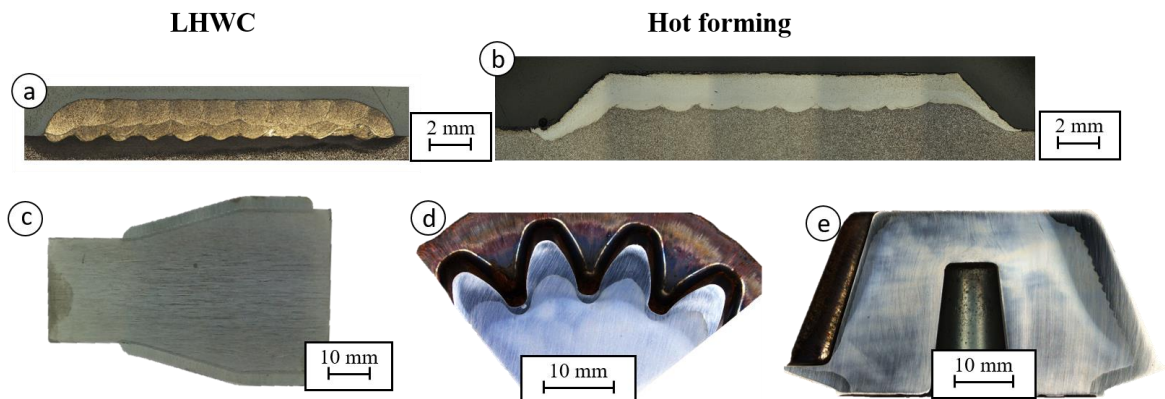


Figure 5: Cladding layer distribution after LHWC and after hot forming: (a) cross-section of a hybrid shaft after LHCW, (b) cross section of a hybrid shaft after CWR, (c) cross-section of a hybrid bevel gear after LHWC, (d) and (e) cross-sections of a hybrid bevel gear after die forging

The example of the shaft with bearing seat can be used to demonstrate the advantages of hot forming with regard to the amount of machining required and the resource efficiency. Figure 6 shows a visualization of the final geometry of the shaft with bearing seat after machining (blue). If this shaft is produced by cladding with subsequent hot forming by CWR, the shaft has an allowance of around 0.5 mm after CWR, which has to be removed by machining (orange). It may be necessary to shorten the shaft at the ends (see Figure 1 (B₃)), but this can be avoided by optimizing the base cylinder geometry. For this investigation, a long base cylinder was chosen to guarantee a complete formation of the shaft geometry, since the focus of the investigation was on the properties of the hybrid components. In further investigations, the base cylinder length can be optimized to ensure minimal rework. If the shaft is produced only by cladding and subsequent machining, the allowance over the shaft is not constant and the machining effort is significantly increased (green). More material has to be removed and is wasted. The amount of waste and machining can be reduced by the hot forming step by manufacturing a near-net-shape part. Reducing the amount of post-processing is of particular interest for materials with poor machinability. The extent to which a reduction in machining effort is possible depends on the target geometry.

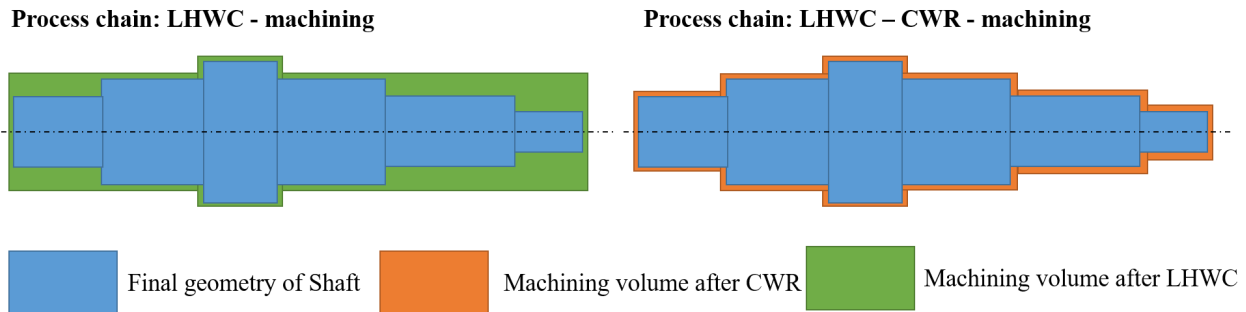


Figure 6: Visualization of the machining volume to reach the final geometry (blue) after CWR (orange) and after LHWC (green)

In the following, the influence of hot forming on microstructure, hardness and residual stresses is demonstrated using the shaft with bearing seat as an example. The hardness curves of the shaft with bearing seat for the different material combinations after LHWC and CWR are shown in Figure 7. For better comparability of the hardness curves, the transition from cladding to base material was chosen as the zero point of the x-axis for the plot. The high-strength claddings have a hardness of 670 to 750 HV0.1 after deposition welding, while the corrosion-resistant AISI 316L cladding has a hardness of only 200 HV0.1. The hardness of the unalloyed carbon steel AISI 1022M ranges from 150 to 200 HV0.1 and the case hardening steel AISI 5120 has a hardness of 200 to 250 HV0.1.

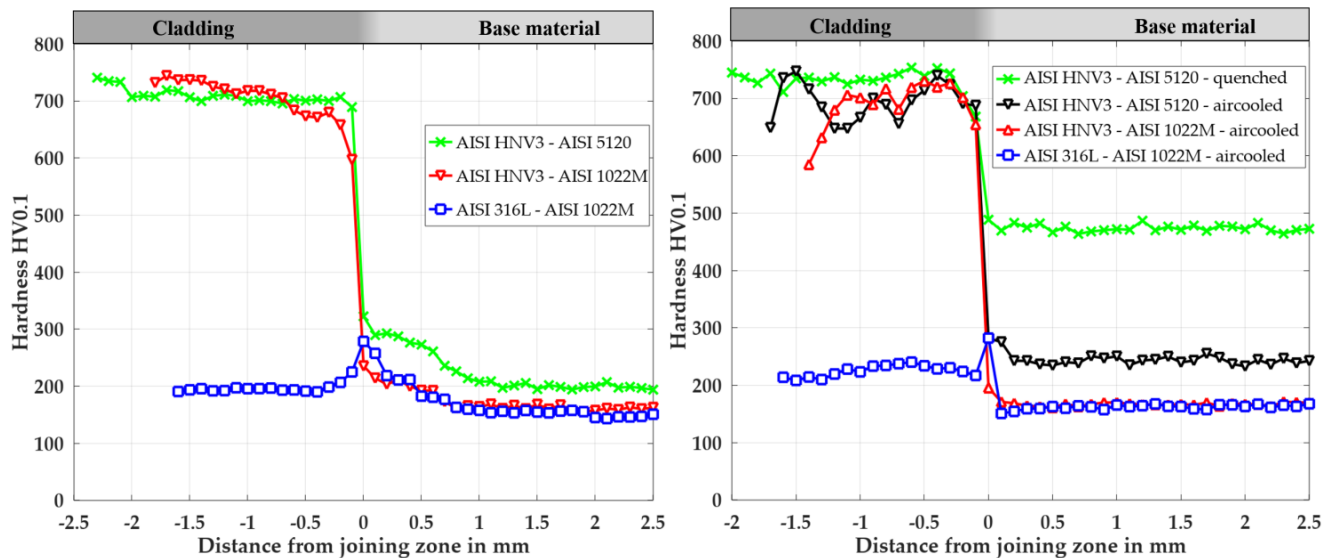


Figure 7: Mean microhardness of the hybrid component with different material combinations after LHWC (left) and after CWR with different cooling strategies (right)

After hot forming the hardness of the AISI 316L is only slightly increased to 200 to 250 HV0.1. The hardness of the unalloyed base material AISI 1022M is in the range of 150 to 170 HV0.1. The samples with a cladding of AISI HNV3 cooled in air show larger hardness variations than the quenched samples. The hardness of the quenched specimens is in the range of 700 to 750 HV0.1 while the hardness of the aircooled specimens is in the range of 650 to 750 HV0.1. A significant increase in hardness is not achieved during quenching, since the cooling rates during air cooling are already sufficient for the formation of a martensitic microstructure. The large hardness variations are caused by scale formation and surface decarburization. The cooling strategy has a great impact on the hardness of the case hardening steel AISI 5120. The hardness of the quenched sample is more than 200 HV0.1 higher than the hardness of the aircooled sample. A hardness of 450 to 500 HV0.1 is achieved in the quenched sample. This indicates that hot forming with air cooling has only a slight effect on the hardness values compared to the cladded condition, while quenching in water can achieve strong increases in hardness depending on the material. For the subsequent application as a bearing seat, a hardness of the cladding of 690 HV +150 HV is targeted. The target hardness is achieved with the quenched samples. For the air-cooled samples, the hardness values fluctuate and are partly below the target value. For these samples, subsequent heat treatment is necessary to reliably achieve the target hardness.

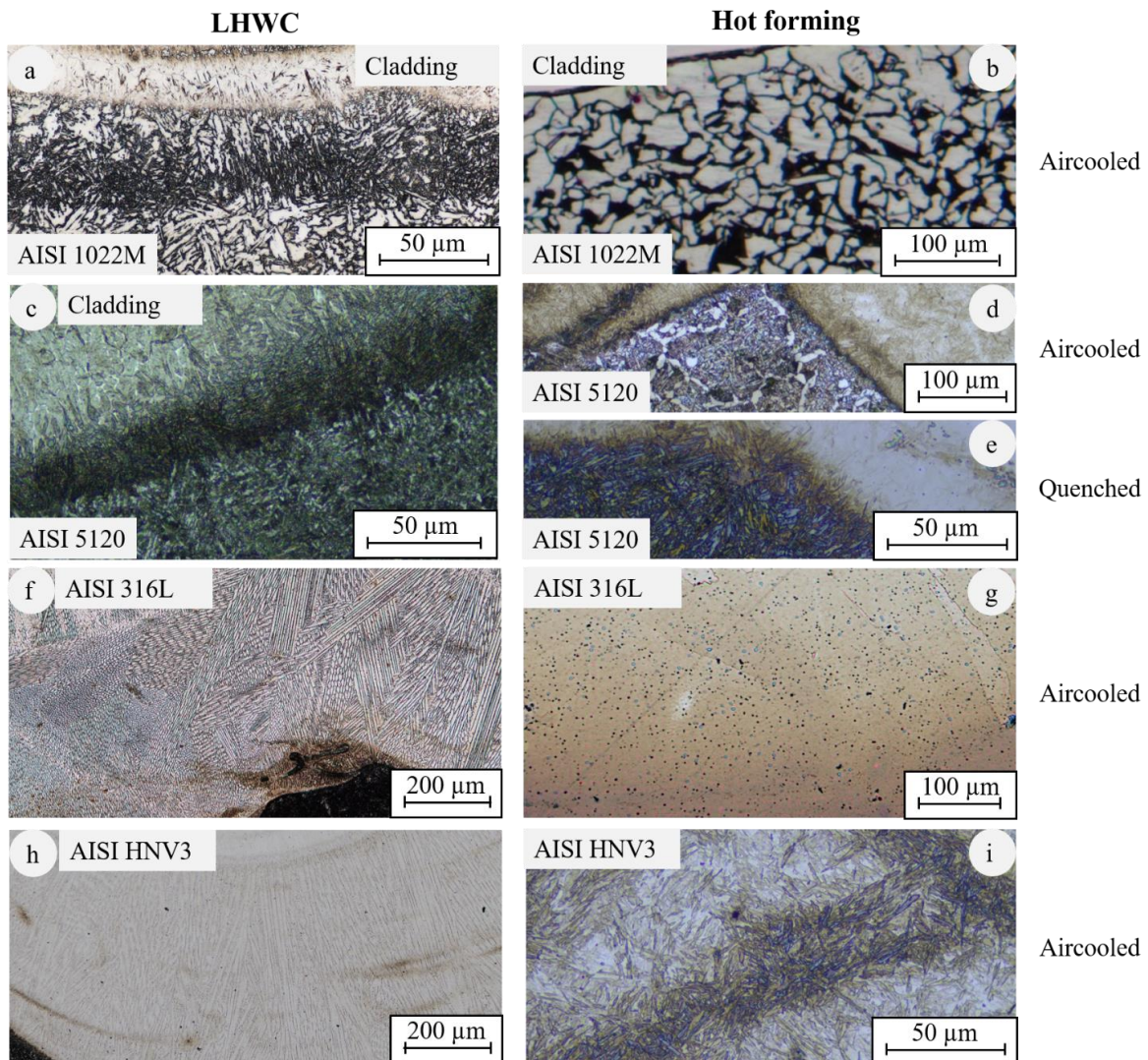


Figure 8: Microstructure after LHWC (a,c,f,h) and CWR (b,d,e,g,i); microstructure of the base material AISI 1022M and AISI 5120 shown in (a,b,c,d,e) and microstructure of the cladding material AISI 316L and AISI HNV3 shown in in (f,g,h,i)

The microstructure after LHWC and hot forming is shown in Figure 8. After LHWC, a Widmannstätten microstructure is present in the base material AISI 1022M (Figure 8 (a)). The base material AISI 5120 has a

ferritic-pearlitic microstructure (Figure 8 (c)). The claddings of AISI HNV3 and AISI 316L have a martensitic and austenitic microstructure, respectively. By applying the second layer of the cladding, the first layer is subjected to heat treatment. Anisotropic microstructure alignment is formed in the first layer (Figure 8 (f) and (h)). After forming, the Widmannstätten microstructure in the base material is transformed into a fine-grained ferritic-pearlitic microstructure ((Figure 8 (b)). Recrystallization by hot forming ensures that there is no longer any anisotropy in the microstructure of the cladding material ((Figure 8 (g) and (i)). The microstructure formation in the AISI HNV3 cladding is independent of the cooling method, but the cooling method influences the microstructure in the AISI 5120 base material. Cooling in ambient air leads to the formation of a ferritic-pearlitic microstructure, while quenching in water leads to the formation of a martensitic microstructure, which contributes to the aforementioned increase in hardness ((Figure 8 (d) and (e)).

A comparison of residual stress in AISI HNV3 and AISI 316L claddings after CWR shows that hot forming influences the residual stress state. The resulting stress state in the cladding depends on the material combination. The residual stress depth profiles after LHWC and CWR are shown in Figure 9. After LHWC, tensile residual stresses occur in the claddings at the surface, changing to the compressive region with increasing distance from the surface. After reaching a compressive residual stress maximum, the residual stresses shift back into the tensile range (AISI 316L cladding) or to lower compressive residual stresses (AISI HNV3).

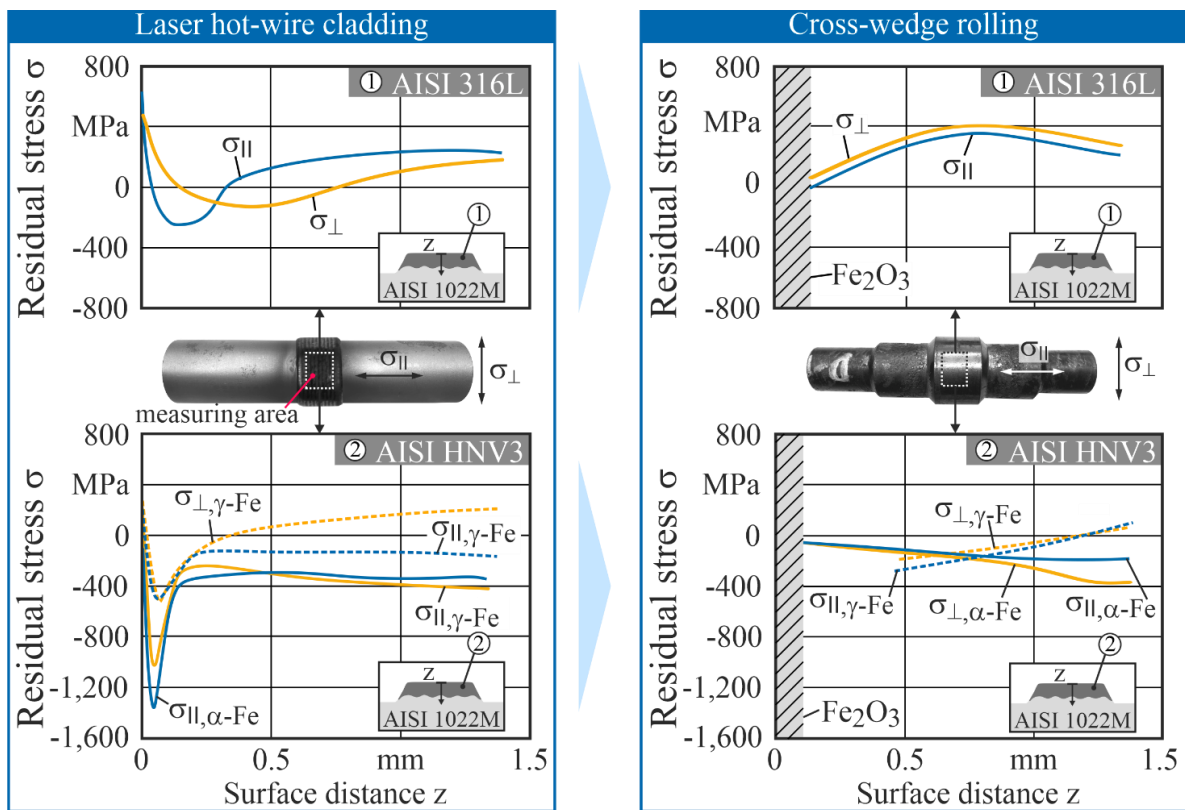


Figure 9: Residual stress depth profile after LHWC and after CWR

The hot forming process has a great influence on the residual stress state. Near-surface residual stress values cannot be measured due to the formation of iron oxide. Residual stresses were measured in the axial and circumferential directions; measurement in the radial direction was not possible with the selected measurement method. The formation of residual stresses after CWR is influenced by three superimposed factors. The deformation of the shaft in radial direction during CWR induces compressive residual stresses into the shaft. The different coefficients of thermal expansion of the cladding and the base material lead to strain incompatibilities during cooling of the hybrid component. This results in the formation of thermophysically induced residual stresses. Since the hybrid components were cooled in air, an inhomogeneous temperature distribution occurred, which can also influence the residual stress formation in the surface and the subsurface area. The residual stresses

in the AISI 316L cladding with a high coefficient of thermal expansion are in the tensile range in both, axial and circumferential directions, after hot forming. The low thermal expansion coefficient of AISI 1022M hinders the shrinkage of the cladding during cooling, and the strain incompatibilities thus lead to the formation of tensile residual stresses in the cladding. After hot forming of the AISI HNV3 cladding, the compressive residual stresses below the surface decrease. Up to a depth of approx. 1.22 mm, compressive residual stresses are present, after which compressive and tensile residual stresses occur.

This shows that the residual stress state after hot forming depends on the selected material combination and that strain incompatibilities between base material and cladding material are the most important factor influencing the residual stress state. If the thermal expansion coefficient of the cladding is greater than that of the base material, tensile residual stresses are formed in the cladding; in the other case, compressive residual stresses are formed. The residual stress state in the cladding after hot forming can thus be influenced by smart material selection. In particular, the option to achieve compressive residual stresses in the high-strength AISI HNV3 cladding is of special interest for component areas with high mechanical/tribological loads, since an increased service life of the cladding can be achieved.

Conclusion and Outlook

In summary, the combination of a cladding process with subsequent hot forming affects the properties of the hybrid component as follows:

- Coarse-grained microstructure and anisotropy in the microstructure are transformed into homogeneous fine-grained forming microstructure by the hot forming process
- For the production of complex geometries such as the bevel gear, simple semi-finished products can be used for the cladding process. The complex geometry is only created in the forming step. The simple semi-finished geometry offers potential for the application of cladding processes with high deposition rates and reduces programming effort and the number of necessary handling axes.
- Hot forming influences the residual stress state in the cladding and, depending on the material combination, advantageous compressive residual stresses can be achieved.
- Depending on the material used, it is possible to harden the hybrid component by quenching from the forging heat.
- The workpiece volume which has to be removed by machining in order to achieve the final geometry can be reduced by mass pre-distribution during hot forming.
- Die forging was used to produce a hybrid bevel gear in which the core of the tooth is made of ductile material and the tooth flank surface is made of high-strength material. In this way, a load-adapted material distribution was realized.

In the next step, the service life of the hybrid components has to be investigated. For this purpose, the bevel gear and the shaft with bearing seat must be machined and, in the case of the air-cooled samples, heat treated. In comparison with cladded components manufactured without hot forming, the positive influence of hot forming on the properties of the hybrid component can be quantified. The investigations can be extended to other material combinations. The combination of an AISI 1022M base material with an intermediate cladding layer of AISI 316L and an outer cladding layer of AISI HNV3 is of particular interest. Due to the strongly different coefficients of thermal expansion of the two cladding materials, it should be possible to achieve compressive residual stresses in the outer cladding layer.

Acknowledgments

This research was funded by the Deutsche Forschungsgemeinschaft (DFG, German Research Foundation) - CRC 1153, subprojects A4, B1, B2, B4 – 252662854.

References

- [1] N. Haghdadadi, M. Laleh, M. Moyle, S. Primig, Additive manufacturing of steels: a review of achievements and challenges, *J. Mater. Sci.* 56 (2021) 64–107. <https://doi.org/10.1007/s10853-020-05109-0>.
- [2] C. Leyens, E. Beyer, Innovations in laser cladding and direct laser metal deposition, in: *Laser Surf. Eng.*, Elsevier, 2015: pp. 181–192. <https://doi.org/10.1016/B978-1-78242-074-3.00008-8>.
- [3] M. Merklein, D. Junker, A. Schaub, F. Neubauer, Hybrid additive manufacturing technologies - An analysis regarding potentials and applications, *Phys. Procedia.* 83 (2016) 549–559. <https://doi.org/10.1016/j.phpro.2016.08.057>.
- [4] V. Ocelík, O. Nenadl, A. Palavra, J.T.M. De Hosson, On the geometry of coating layers formed by overlap, *Surf. Coatings Technol.* 242 (2014) 54–61. <https://doi.org/10.1016/j.surfcoat.2014.01.018>.
- [5] D. Ding, Z. Pan, D. Cuiuri, H. Li, A multi-bead overlapping model for robotic wire and arc additive manufacturing (WAAM), *Robot. Comput. Integr. Manuf.* 31 (2015) 101–110. <https://doi.org/10.1016/j.rcim.2014.08.008>.
- [6] O. Nenadl, V. Ocelík, A. Palavra, J.T.M. De Hosson, The prediction of coating geometry from main processing parameters in laser cladding, *Phys. Procedia.* 56 (2014) 220–227. <https://doi.org/10.1016/j.phpro.2014.08.166>.
- [7] D. Junker, O. Hentschel, M. Schmidt, M. Merklein, Investigation of Heat Treatment Strategies for Additively-Manufactured Tools of X37CrMoV5-1, *Metals (Basel).* 8 (2018) 854. <https://doi.org/10.3390/met8100854>.
- [8] J. Hafenecker, C.-M. Kuball, R. Rothfelder, M. Schmidt, M. Merklein, Surface modification of additively manufactured parts by forming, *ESAFORM 2021.* 13 (2021) 1–12. <https://doi.org/10.25518/esaform21.2124>.
- [9] C. Li, Z.Y. Liu, X.Y. Fang, Y.B. Guo, Residual Stress in Metal Additive Manufacturing, *Procedia CIRP.* 71 (2018) 348–353. <https://doi.org/10.1016/j.procir.2018.05.039>.
- [10] A. Franceschi, J. Stahl, C. Kock, R. Selbmann, S. Ortmann-Ishkina, A. Jobst, M. Merklein, B. Kuhfuß, M. Bergmann, B.A. Behrens, W. Volk, P. Groche, Strategies for residual stress adjustment in bulk metal forming, *Arch. Appl. Mech.* 91 (2021) 3557–3577. <https://doi.org/10.1007/s00419-021-01903-7>.
- [11] Voestalpine Böhler Welding Nederland B.V., Inspection certificate 3.1 UTP A DUR 600, 2021.
- [12] Metal Technology - Canterbo GmbH, Abnahmeprüfzeugnis 3.1 MT-316L 1.4430, 2019.
- [13] Deutsche Edelstahlwerke Services GmbH, 1.7147/1.7149 - 20MnCr5/20MnCrS5, (2011). https://www.dew-stahl.com/fileadmin/files/dew-stahl.com/documents/Publikationen/Werkstoffdatenblaetter/Baustahl/1.7147_1.7149_de.pdf (accessed August 4, 2021).
- [14] Matmatch, Matmatch EN 10273 Grade P250GH normalized or normalized formed (+N), (n.d.). <https://matmatch.com/de/materials/minfm35728-en-10273-grade-p250gh-normalized-or-normalized-formed-n->.
- [15] Z. Pater, Cross-Wedge Rolling, in: *Compr. Mater. Process.*, Elsevier, 2014: pp. 211–279. <https://doi.org/10.1016/B978-0-08-096532-1.00315-0>.
- [16] B.-A. Behrens, A. Chugreeva, J. Diefenbach, C. Kahra, S. Herbst, F. Nürnberger, H.J. Maier, Microstructural Evolution and Mechanical Properties of Hybrid Bevel Gears Manufactured by Tailored Forming, *Metals (Basel).* 10 (2020) 1365. <https://doi.org/10.3390/met10101365>.
- [17] L. Budde, V. Prasanthan, P. Merkel, J. Kruse, M.Y. Faqiri, M. Lammers, M. Kriwall, J. Hermsdorf, M. Stonis, T. Hassel, B. Breidenstein, B.-A. Behrens, B. Denkena, L. Overmeyer, Material dependent surface and subsurface properties of hybrid components, *Prod. Eng.* (2022). <https://doi.org/10.1007/s11740-022-01128-9>.
- [18] L. Budde, V. Prasanthan, J. Kruse, M.Y. Faqiri, M. Lammers, J. Hermsdorf, M. Stonis, T. Hassel, B. Breidenstein, B.-A. Behrens, B. Denkena, L. Overmeyer, Investigation of the influence of the forming process and finishing processes on the properties of the surface and subsurface of hybrid components, *Int. J. Adv. Manuf. Technol.* 119 (2022) 119–136. <https://doi.org/10.1007/s00170-021-08066-3>.